colloids and interfaces

MDPI

Article

Electrochemical Perspective on Hematite–Malonate Interactions

Karolina Kędra [1,*], Marzena Łazarczyk [1], Tajana Begović [2], Danijel Namjesnik [2], Karolina Lament [3], Wojciech Piasecki [4] and Piotr Zarzycki [1,5]

1 Institute of Physical Chemistry, Polish Academy of Sciences, 01-224 Warsaw, Poland; mprus@ichf.edu.pl (M.Ł.); zarzyckipiotrek@gmail.com (P.Z.)
2 Department of Chemistry, Faculty of Science, University of Zagreb, Horvatovac 102a, 10000 Zagreb, Croatia; tajana.begovic@pmf.unizg.hr (T.B.); danijel.namjesnik@pmf.unizg.hr (D.N.)
3 Regional Research and Development Center, Józef Piłsudski University of Physical Education in Warsaw, 21-500 Biała Podlaska, Poland; karolina.lament@awf.edu.pl
4 Faculty of Physical Education and Health, Józef Piłsudski University of Physical Education in Warsaw, 21-500 Biała Podlaska, Poland; wojciech.piasecki@awf.edu.pl
5 Energy Geosciences Division, Lawrence Berkeley National Laboratory, 1 Cyclotron Road, Berkeley, CA 94720, USA
* Correspondence: kkedrakrolik@ichf.edu.pl

Abstract: Organic matter (OM) interactions with minerals are essential in OM preservation against decomposition in the environment. Here, by combining potentiometric and electrophoretic measurements, we probed the mode of coordination and the role of pH-dependent electrostatic interactions between organic acids and an iron oxide surface. Specifically, we show that malonate ions adsorbed to a hematite surface in a wide pH window between 3 and 8.7 (point of zero charge). The mode of interactions varied with this pH range and depended on the acid and surface acidity constants. In the acidic environment, hematite surface potential was highly positive (+47 mV, pH 3). At pH < 4 malonate adsorption reduced the surface potential (+30 mV at pH 3) but had a negligible effect on the diffuse layer potential, consistent with the inner-sphere malonate complexation. Here, the specific and electrostatic interactions were responsible for the malonate partial dehydration and surface accumulation. These interactions weakened with an increasing pH and near PZC, the hematite surface charge was neutral on average. Adsorbed malonates started to desorb from the surface with less pronounced accumulation in the diffuse layer, which was reflected in zeta potential values. The transition between specific and non-specific sorption regimes was smooth, suggesting the coexistence of the inner- and outer-sphere complexes with a relative ratio that varied with pH.

Keywords: ion adsorption; dicarboxylate ions; iron oxide α-Fe_2O_3; hematite; electrical double layer; surface potential; ζ-potential

Citation: Kędra, K.; Łazarczyk, M.; Begović, T.; Namjesnik, D.; Lament, K.; Piasecki, W.; Zarzycki, P. Electrochemical Perspective on Hematite–Malonate Interactions. *Colloids Interfaces* **2021**, *5*, 47. https://doi.org/10.3390/colloids5040047

Academic Editor: Agnieszka Ewa Wiacek

Received: 30 September 2021
Accepted: 29 October 2021
Published: 31 October 2021

1. Introduction

The quality of soil depends primarily on its organic matter content [1]. The interactions of soil organic matter (SOM) with minerals governs the SOM preservation in soil, but these interactions are still poorly understood [2,3]. One of the SOM preservation mechanisms relies on SOM adsorption to mineral surfaces, which apparently limits microbial decomposition. However, it remains a challenge to identify the actual modes of SOM protection by mineral surfaces because many phenomena may contribute, ranging from the SOM aggregates or co-precipitates with mineral phase to structural and physicochemical changes in SOM induced by interactions with minerals that disable some degradation pathways [4,5]. Those mechanisms set apart OM from decomposing biota, as well as limiting oxygen diffusion [6]. Organic matter preservation is a complex phenomenon. There is a need to consider two potentially important parallel processes, i.e., the restriction of microbial access to organic matter accumulated near the mineral surface, and organic matter sorption to the mineral surface [2–4,6].

Here, we focus on understanding the nature of OM interactions with mineral surfaces from the electrochemical perspective. One of the open questions regards the SOM sorption mode to mineral surfaces (e.g., carbonates, iron oxides, clays, silicates) [2,4,6,7]. Decades of studies have shown that modes of sorption vary with environmental conditions, such as pH, ionic strength, temperature, depth of deposition, and oxic/anoxic conditions, as well as type functional groups exposed by the OM and mineral surface.

This work focused on one of the most stable and common iron oxide mineral, hematite [8,9], and a simple dicarboxylic acid, malonate. The latter is considered a prototypical SOM. We chose hematite because of its dual action in SOM-preservation. Under oxic conditions, the SOM is preserved by adsorption or co-precipitation with iron minerals. However, under anoxic conditions, Fe(III) solid ions are able to oxidize SOM, thus facilitating SOM degradation [4]. We chose malonate due to its abundance in SOM moiety secreted by plant roots into the rhizosphere [10] and its presence in atmospheric aerosols [11].

In this study, we present an insight into hematite–malonate interactions by combining three electrochemical descriptors of the electrical double layer formed at the mineral/electrolyte interface: (a) surface potential, (b) surface charge density, and (c) zeta-potential [12–24]. We gain new insight into the pH-dependent malonate interaction with hematite by examining the pH-dependent surface charge, diffuse layer potential, and surface potential. Our results are important because they illustrate that SOM-mineral interactions are dictated by the pH-controlled charge state of mineral surface and SOM functional groups.

2. Materials and Methods

2.1. Materials

Hematite (α-Fe_2O_3) nanoparticles (diameter 20–40 nm, purity 98%) were from US Research Nanomaterials, Inc. We prepared a hematite (α-Fe_2O_3) single crystal electrode with only the (001) crystallographic orientation [25]. The artificially made hematite crystal with dimensions of 5 mm × 5 mm and a thickness of 0.5 mm for the construction of the electrode, was from SurfaceNet GmbH, Rheine, Germany. The crystal was cut and epi-polished by the manufacturer. The electrode surface exposed to the solution was only (001) hematite face (SI, Figure S1a). Malonic acid was 99% pure from ReagentPlus. Speciation of the malonic acid in the bulk of the solution was characterized by pK_{a1} = 2.83 and pK_{a2} = 5.69 [26]. Other chemicals were of analytical reagent grade. All solutions were prepared using MilliQ water (18.2 MΩ cm).

2.2. Methods

2.2.1. Potentiometric Acid–Base Titration

We performed the alkalimetric titration using a Metrohm Titrando 907 apparatus according to the conventional procedure with respect to recommendations for obtaining comparable results [24,27]. All the measurements were carried out under an argon atmosphere using freshly prepared, degassed, and thermostated at 25 °C suspensions to avoid oxidation. We applied a combined glass electrode (Unitrode from Metrohm, Herisau, Switzerland) to measure pH, with a drift limit established to be below 0.5 mV/min. We carried out the alkalimetric titration by the addition of a titrant (40 µL of 0.1 mol dm^{-3} NaOH), as only the glass-electrode potential was stabilized.

We determined proton surface charge density (σ_H) by the use of potentiometric acid–base titration of hematite suspension and calculated from the equation [24,28,29].

$$\sigma_H = \frac{F}{A_s C_s}\left[\left(\frac{c_{HCl}\Delta V_{HCl}}{V_{susp}} - \frac{10^{-pH}}{\overline{\gamma_\pm}}\right) - \left(\frac{c_{NaOH}\Delta V_{NaoH}}{V_{susp}} - \frac{10^{pH-14}}{\overline{\gamma_\pm}}\right)\right] \quad (1)$$

where F is Faraday constant, A_s is hematite specific surface area (m^2 g^{-1}), C_s is hematite mass concentration in suspension (g dm^{-3}); c_{HCl} and c_{NaOH} are the concentrations of HCl and NaOH in aqueous solutions, ΔV_{HCl}, ΔV_{NaOH} is the added volume of HCl and NaOH;

$\overline{\gamma_{\pm}}$ is the mean activity coefficients, and V_{susp} is suspension volume. The mean activity coefficients were determined using the Davies formula [30].

If the solid sample does not contain any impurities, or no specific adsorption takes place, the net proton surface charge corresponds to the surface charge density ($\sigma_H = \sigma_0$), and the net proton zero surface charge corresponds to the point of zero charge ($pH_{npzc} = pH_{pzc}$) [31].

The mass concentration of hematite for all titrations was 10 g dm^{-3}, and the aqueous electrolyte solution consisted of NaCl 10^{-3} mol dm^{-3}.

2.2.2. Electrokinetic Measurements

For electrokinetic measurements, we used stock suspension of 10 g dm^{-3} hematite nanoparticles dispersed in 10^{-3} mol dm^{-3} HCl solution (pH = 3). Hematite slurry at a volume of 5 mL was added to freshly prepared and degassed electrolyte solution at pH 3. If the pH value changed due to the surface protonation, we brought it back to pH = 3 by adding HCl. The final solid concentration of the samples measured after several hours of equilibration was equal to 0.5 g dm^{-3}.

The ζ potential of hematite nanoparticles was measured using a Zetasizer Nano ZS Malvern at 25 °C. Measurements were performed before and after adsorption of malonic acid in three different concentrations for a hematite nanoparticles suspension (0.5 g dm^{-3}). The hematite suspensions were titrated using 0.1 M NaOH in a pH range from 3 to 10. Electrokinetic potential of hematite suspension was also examined in a function of ionic strength of electrolyte (NaCl and malonates) (SI, Figure S2).

2.2.3. Surface Potential Measurements

We measured the open circuit potentials of the cell composed of hematite (001) single crystal electrode (SCrE) [12,15,16,32] and the reference electrode Ag | AgCl | KCl (3 mol dm^{-3}) using a combined pH microelectrode (Metrohm). The SCrE electrode consisted of a single hematite crystal connected to a copper wire using conductive silver paint. The hematite crystal was glued to an acrylic holder with nonconductive UV-curable epoxy glue. The copper wire was connected to the pH meter via shielded cables. All other sides of the crystal except for the front (001) side were insulated by using the same (nonconductive) glue. We used two pH meters (Metrohm) for the measurement of the pH and the SCrE potentials. The SCrE was connected to one pH meter and the combined pH electrode to another. The reference electrode inside the combined electrode was used as a standard reference electrode for SCrE measurements too (SI, Figure S1b).

Before the use, we rinsed the crystal surface with ethanol and deionized water. Then, we performed titrations with different concentrations of malonic acid. The SCrE with combined pH microelectrode was immersed into a thermostated glass cell containing 30 mL of 1×10^{-3} mol dm^{-3} HCl, 1×10^{-3} mol dm^{-3} NaCl, and malonic acid. The solution was degassed with argon (Ar 5.0, Messer). The desired pH values were achieved by adding 0.1 mol dm^{-3} NaOH to the solution. The measured SCrE potential was monitored in real-time by using the infrared link between the pH meter and the computer. The data were collected in 4 s intervals by using RS232 DataLogger 2.7 (Eltima Software). Upon each addition, the solution was stirred by a magnetic stirrer. The measurements were made after achieving equilibrium, which was 10–20 min after each addition of NaOH. The equilibrium was assumed when the slope of the measured potential was below 1 mV min^{-1}.

The extraction of the absolute values of the surface potential from the measurements is not trivial [15,33–35]. In order to obtain the surface potential at the hematite/electrolyte interface from the measured open-circuit potential, one needs to account for all potential jumps in the electrochemical cell [15,33–35]. The zero level of inner surface potential (p.z.p., $\Psi_0 = 0$) is located between $p\mathrm{H}_{pzc}$ and $p\mathrm{H}_{iep}$ values [32]. In this work, the value of $p\mathrm{H}_{pzp}$ was determined to be equal to 8.7.

The SCrE potential measurements were used to monitor the surface potential response to detachment, complexation, and reduction in the surface iron sites.

3. Results and Discussion

3.1. Surface Charge of Hematite

The surface of hematite becomes charged due to proton uptake and release by the surface-exposed oxygen atoms or due to dissociative water sorption [36]. Surface properties of metal oxides, and thus hematite, are pH-dependent. Potential determining ions for hematite in aqueous solution are H^+ and OH^-. Thus, the point of zero charge ($\sigma_H = 0$) in this system is determined by the pH of the bulk of the solution. Surface reactivity, average surface equilibrium constants, point of zero charge, and isoelectric point vary for hematite samples of different origin and impurity [37]. What is more, the binding of carboxylic acid to the hematite surface affects both the electrostatic interfacial properties and overall surface stability, triggering hematite (photo)dissolution [38,39].

For the determination of pH_{pzc}, we performed a series of alkalimetric potentiometric titrations of hematite slurries with three different ionic strengths of electrolyte and calculated the proton surface charge densities using Equation (1). The plots of proton surface charge density are shown in Figures 1a and 2. Three curves for three different ionic strengths in Figure 2 did not intersect at one point, but the pH region between 8.5 and 8.9 was noticed. The presence of the common intersection point (CIP) [40] is essential for the accurate determination of the PZC; still, we were able to estimate PZC as a mean value of pH in the region of the intersections of all curves (pH_{pzc} = 8.7). The surface charge σ_0 was calculated taking into account acidic impurities from the synthesis (HCl), as described by Piasecki et al. [28].

(**a**)

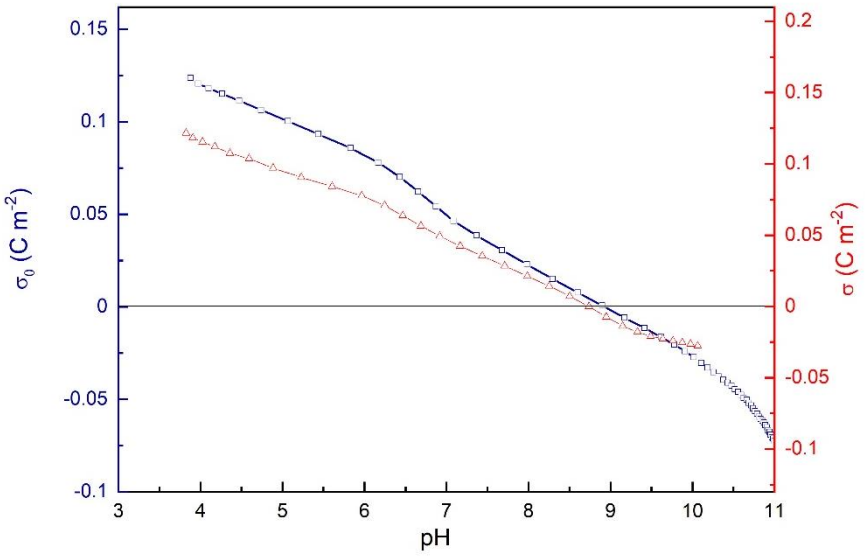

Figure 1. *Cont.*

(**b**)

(**c**)

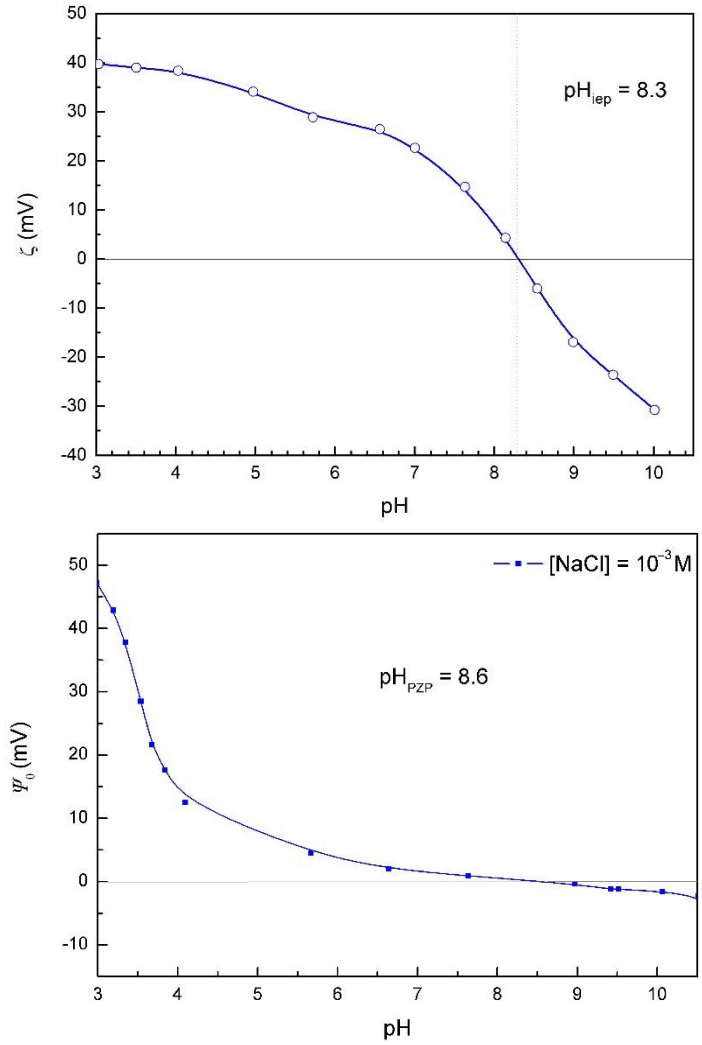

Figure 1. Electrochemical characteristics of hematite suspension as a function of pH: (**a**) net surface charge and proton surface charge densities in 10^{-3} mol dm^{-3} NaCl; (**b**) electrokinetic potential of hematite in 10^{-3} mol dm^{-3} NaCl; (**c**) hematite surface potential (Ψ_0) as a function of pH in 10^{-3} mol dm^{-3} NaCl at 25 °C.

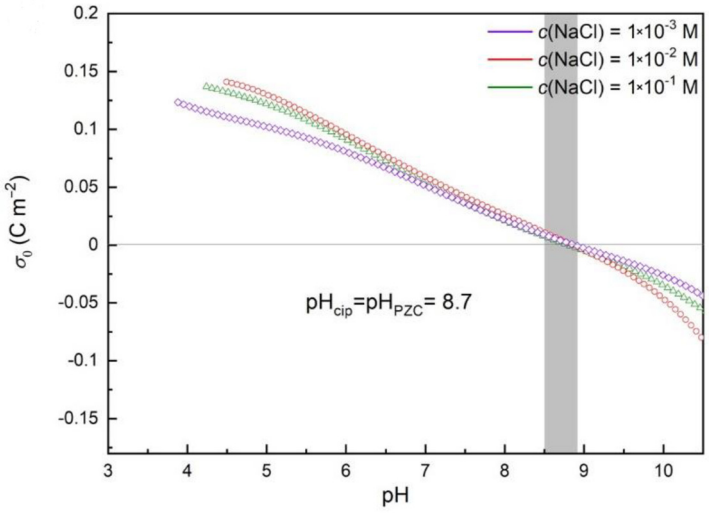

Figure 2. Net surface charge of hematite dispersed in pure electrolyte. Surface charge density as a function of pH for different concentrations of NaCl: 10^{-3} mol dm^{-3} NaCl, 10^{-2} mol dm^{-3} NaCl, and 0.1 mol dm^{-3} NaCl.

3.2. Zeta and Surface Potential

The isoelectric point of hematite particles was obtained from the zeta potential measurements (Figure 1b), pH_{iep} = 8.3. The difference in pH_{pzc} and pH_{iep} of hematite particles in sodium chloride aqueous solution indicates that chloride ions exhibited higher affinity for association with positively charged hematite surface than sodium ions [41].

Surface potentials at the hematite/electrolyte interface (Figure 1c) were evaluated from measured hematite (001) single crystal electrode potentials under the assumption that a point of zero potential corresponds to the average value of the isoelectric point and point of zero charge, pH_{pzp} = 8.6. The surface potential does not obey the quasi-Nernstian law, which is evidence of the nonlinear effects and expected for the hematite (001) surface [36,42].

The surface charge and surface potential of hematite depend on the pH and electrolyte concentration. Due to the association of counterions and possible adsorption of some other species, the surface charge determined via potentiometric titration is called the effective surface charge.

The charged hematite surface attracts counterions from the aqueous solution and binds various species. The amount and strength of the adsorption depend on hematite surface properties as well on charge and structure of adsorbing species. Finally, the adsorbed species change hematite surface properties.

The value of pH_{pzp} was close to the obtained pH_{pzc}, shifted in the opposite direction from pH_{iep}, so that $pH_{iep} < pH_{pzp} \leq pH_{pzc}$.

3.3. Malonates Effect on Hematite Surface Charge Density

Figure 3 shows the influence of malonate anions on the proton surface charge densities in the suspension of hematite with and without malonic acid. The point of zero charge obtained from the acid–base potentiometric titration of hematite suspension without malonate (blue line in Figure 3) was found to be at pH_{pzc} = 8.7, the same as was determined from the common intersection point of the three curves obtained for three different ionic strengths (Figure 1a). The results shown in Figure 3 indicate a shift of the hematite n.p.z.c. to the higher pH values with the increasing concentration of malonate (SI, Figure S4). The malonate anions strongly affected the electrokinetic potential of α-Fe_2O_3 particles (see Figure 4), making zeta-potential more negative compared with the pure oxide/NaCl electrolyte suspension.

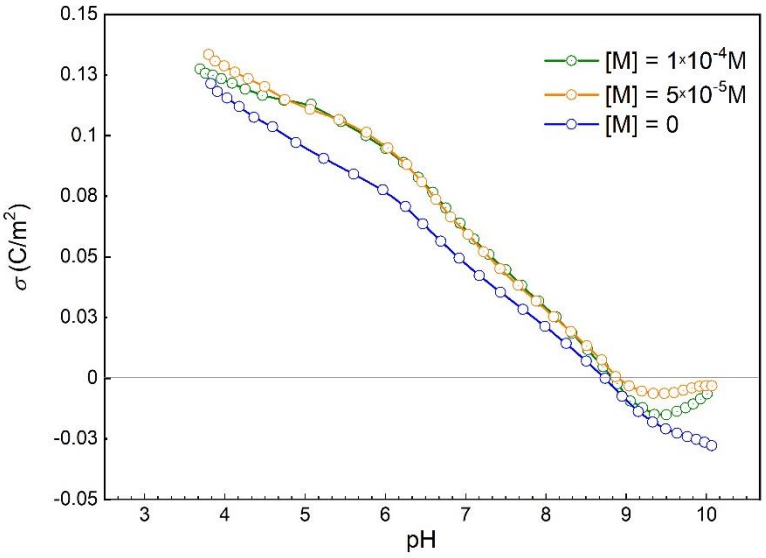

Figure 3. Proton surface charge densities of hematite in the suspension of hematite in 10^{-3} mol dm^{-3} NaCl: without malonic acid (blue line) and with 5 × 10^{-5} mol dm^{-3} malonic acid (orange line), 10^{-4} mol dm^{-3} malonic acid (purple line) at 25 °C.

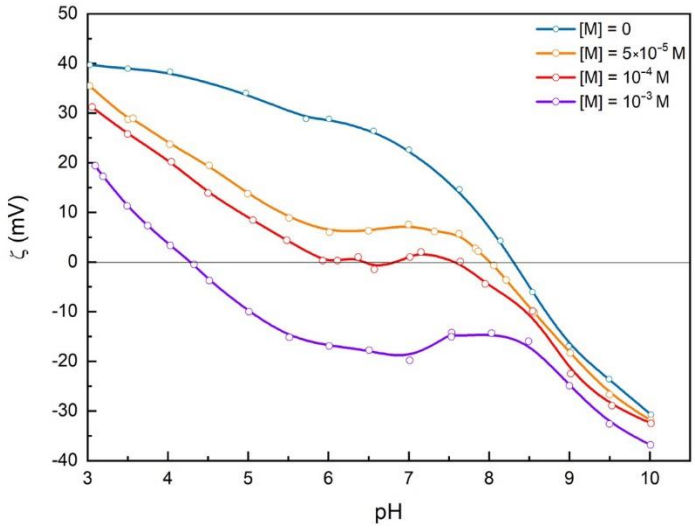

Figure 4. Effect of malonate ions concentration on the electrokinetic potential of hematite particles dispersed in 10^{-3} mol dm^{-3} NaCl at 25 °C.

3.4. Malonates Effect on Zeta Potential

The results of electrokinetic measurements indicate that malonates adsorb at the hematite surface (see Figure 4). Above pH 8.6, the hematite surface is negatively charged, and malonate sorption is not expected, which is consistent with the similar values of zeta potential obtained in this pH region, irrespective of the malonate concentration. Binding of malonates shifts the hematite isoelectric point to a lower pH. This effect is opposite to the shift of n.p.z.c. (see "SI, Figure S4"), confirming the specific adsorption of malonates at the hematite surface.

Moreover, ζ(pH) curves for hematite slurries with a high concentration of malonic acid are specific in shape with a plateau between pH 5.7 and pH_{iep}. The appearance of the plateau can be explained considering several effects of malonates on the hematite surface. The fraction of different malonate spices (H_2A, HA^-, and A^{2-}, see "Figure 5"), as well as hematite surface charge, are pH-dependent. Hematite surface is positively charged in the acidic region up to the point of zero charge and isoelectric point. Below pH < 5.5 in the bulk of the aqueous solution, the number of HA^- ions on the positively charged hematite surface increases. Above pH > 4, the concentration of A^{2-} ions gradually increases, and adsorption of A^{2-} ions on the still positively charged hematite surface occurs. In the pH range 4 < pH < 5.5 competitive adsorption can be expected. In this pH region, a specific shape of Ψ_0(pH) curve for hematite surface without adsorbed malonates ions (Figure 3) was found. The broad plateau near the point of zero potential and relatively high positive potential at pH < 5 affect the adsorption of malonate species and shape of the ζ(pH) curves.

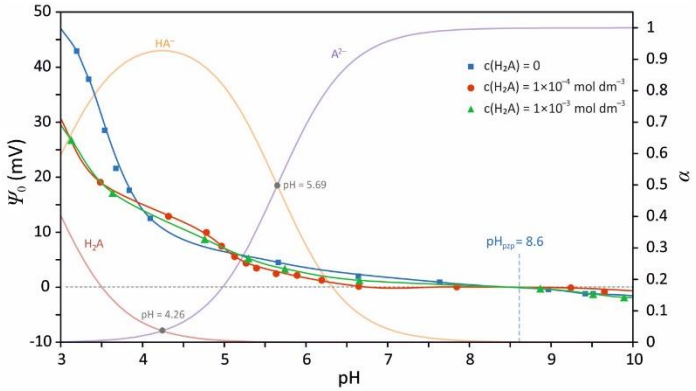

Figure 5. The effect of malonate ions adsorption on the inner surface potential of (001) hematite surface at 25 °C. The overlaid speciation diagram of malonic acid was made using pK_{a1} = 2.83, pK_{a2} = 5.69 [26], and Visual MINTEQ ver. 3.1.

The observed effects indicate strong electrostatic interactions of positively charged hematite surface with malonates and formation of inner-sphere complexes. At higher pH, the hematite surface is neutral or negatively charged, and weaker interactions lead to reduced malonate adsorption. However, the binding of divalent A^{2-} ions to hematite surface prevails, which causes a charge compensation and reduction in the mobility of the particle.

3.5. Insight into Malonates Sorption Modes

Despite decades of studies [38,43,44], coordination modes are still puzzling. A few infra-red spectroscopic studies reveal either one of two types of surface complexes: inner- and outer-sphere bidentate complexes of malonates at Fe(III) oxide/aqueous electrolyte 245 interface [38,43,44]. Persson et al. [43] and Lenhart et al. [44] showed that in the acidic solution (pH < 5.5), the inner-sphere complexes are expected, while the outer-sphere complexes should dominate at higher pH. However, others have observed only inner-sphere bidentate complexes [38]. One of the limitations of previous studies is a lack of electrochemical probes of malonate's effect on the electrical double layer formed at the hematite/electrolyte interface. Our results described above suggest that the nature of the hematite–malonate interactions drastically changes around pH 5, in agreement with IR spec-252 troscopic and adsorption studies [43,44]. We concluded that at least two types of surface malonate complexes exist on the hematite surface: strongly bound malonate in the inner-sphere complex geometry at lower pH, and outer-sphere and mobile complex at higher pH.

The surface potential measurements by means of hematite (001) single crystal electrode shed extra light on the nature of binding of malonic acid species to the hematite (001) surface. Figure 5 presents the variation of surface potential with pH for three different concentrations of malonic acid. The overlaid speciation diagram (Figure 5) shows that below pH 4 in the aqueous solution is present fully protonated malonic acid (H_2A). At that pH, the hematite surface is predominantly occupied by protonated bridging oxygen—OH_2^+ groups. The adsorption of malonic acid decreases the surface potential at pH below 4. Above pH above 4 the adsorption of malonate has almost no effect on surface potential. The change in the surface potential sensitivity to sorption of malonate is a clear indication of the change in the coordination mode from the inner-sphere (close proximity) at low pH to the outer-sphere (far from the surface) at higher pH.

Clearly, there is a correlation in surface charge shift and malonate speciation (Figure 5). Although HA^- dominates at pH below 4, the surface potential is negatively correlated with HA^- concentration.

3.6. Coexistence of Various Coordination Modes

Our findings suggest a coexistence of different types of bonding of carboxylic groups to the hematite surface (Figure 6). At low pH < PZC but above pK_{a1}, the dominant speciation of malonic is HA^- and hematite surface is positively charged. In this case we observe inner-sphere sorption with strong electrostatic interactions. At pH near PZC, surface charge is neutral on average, and A^{2-} is dominant above pK_{a2}, and there is weak sorption via hydrogen-bonding with water mediating interactions (outer sphere coordination) or less frequent inner-sphere coordination with a few remaining positively charged sites. At high pH above PZC, hematite surface is negatively charged and malonic is deprotonated (A^{2-}) so direct surface–malonate interactions are energetically unfavorable due to electrostatic repulsion, but the indirect interactions via a hydrogen-bonded chain of water molecules or ion-pairing with the surface adsorbed Na^+ are possible. The extent of sorption decreases with increasing pH, along with a shift in coordination modes.

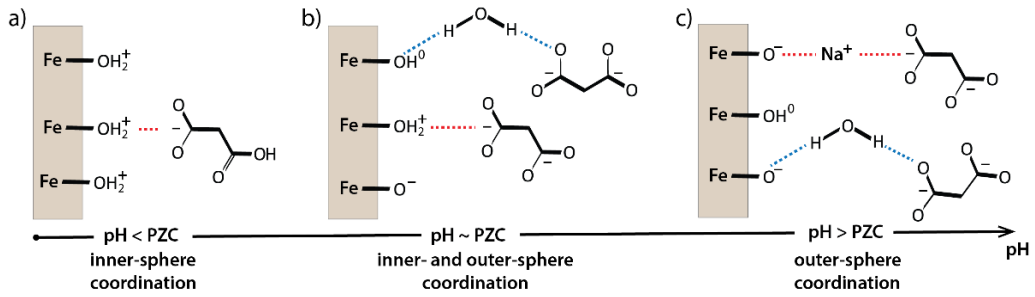

Figure 6. Hematite–MA interactions. (**a**) Low pH < PZC but above pK_{a1}, surface positively charged inner-sphere sorption with strong electrostatic interactions; (**b**) pH near PZC, surface charge neutral on average, weak sorption via hydrogen-bonding, with water mediating interactions (outer sphere coordination) or eventually inner-sphere coordination with a few remaining positively charged sites; and (**c**) high pH above PZC, the indirect interactions via a hydrogen-bonded chain of water molecules or ion-pairing with the surface adsorbed Na^+.

Due to the small reactive hematite surface area, the difference between hematite surface potential at two different malonic acid concentrations (1×10^{-3} and 1×10^{-4} M) was negligible (see "Figure 5").

Malonates adsorbed at hematite surface decreased the inner surface potential above pH < 4, which influenced the distribution of ions within the interfacial layer. In this pH region, electrokinetic potential was just slightly affected by malonate adsorption, while surface charge density differed significantly. This indicates the formation of malonate surface complexes at the hematite surface below pH 4. Due to the adsorption of fully protonated malonic acid, the inner surface potential of hematite decreased. Adsorption of malonic acid caused adsorption of some protons from the hematite surface, which was obtained with sequences of adding of malonates and hematite to the electrolyte (SI Figure S3).

4. Conclusions

The interactions between soil/dissolved organic matter and charged minerals govern the stability of OM in the environment. There are many different modes of interaction, but sequestration of OM via sorption to mineral surfaces is often the initial step in the protective and destructive function of minerals.

Here we present the electrochemical study of malonate binding to hematite surface by combining surface charge, surface potential, and diffuse layer measurements. We observed that malonate ions bind to the surface of hematite in a wide pH range but that the mode and strength of this interaction varied with pH. Under acidic conditions, malonates were specifically adsorbed to positively charged oxide surface. In this regime, malonate was

adsorbed as an inner-sphere complex because the surface charge and potential but not the diffuse layer potential were sensitive to malonate concentration.

At higher pH (>5), malonates started to detach from the hematite surface and accumulated near the shear plane of the EDL. The malonate became non-specifically adsorbed as the outer-sphere complex and preferentially accumulated in the diffuse layer, affecting ζ-potential with a negligible effect on the surface charge/potential. The transition from the inner- to outer-sphere complex geometries appeared to be smooth, suggesting that both modes of coordination existed simultaneously. However, their relative ratio varied with the solution pH.

We showed that a combination of different electrochemical techniques provided unique insight into the coordination and location of adsorbed species within the EDL. Our findings are in agreement with previous spectroscopic studies [38,43,44], but they provide additional information about how EDL is affected by malonate sorption. Formation of inner-sphere complexes involves strong electrostatic interactions, partial dehydration of ligands, and presumably formation of chemical bonds [38,43,44]. The amount of malonate ions in the diffuse layer increased with increasing pH, as indicated by the variation of the ζ-potential. At the same time, the amount of the specifically adsorbed malonate in the rigid part of the EDL decreased, as indicated by decreasing sensitivity of surface charge and potential to the varying concentration of malonate.

From the mineral surface perspective, specifically adsorbed malonic ligands leaving hematite surface can detach with the iron ion, driving the ligand-assisted mineral dissolution. Our study suggests that pH-dependent change in the carboxylic acid surface coordination is one of the first steps in the ligand-promoted iron oxide dissolution and is relevant for the mobilization of iron and other contaminants in the environment.

From the organic matter perspective, the interfacial structure and preservation of SOM was to some extent driven by sorption and immobilization of organic matter at the hematite surface; however, these complexes are often photoactive or act as stronger oxidants/reductants, which is vital for catalyzing SOM degradation near iron oxide surfaces [45–47].

Supplementary Materials: The following are a vailable online https://www.mdpi.com/article/10.3390/colloids5040047/s1, Figure S1: Schematic presentation of hematite (001) single crystal electrode (SCrE), (a) and a cell composed of hematite and reference electrodes for surface potential response monitoring (b); Figure S2: Electrokinetic potential of hematite suspension as a function of ionic strength of NaCl/MA electrolyte; Figure S3: pH changes response in two sequences ofadditions of malonates and hematite; Figure S4: Effect of malonate ions concentration on pHnpzcand pHiepof hematite; Figure S5. Proposed reactions of adsorption of malonic acid and malonate to the hematite (001) surface for two types of bonding, bidentate mononuclear (a), (c), and bidentatebinuclear (b), (d) at pH lower than 4 (a), (b), and for pH between 4 and 7 (c), (d). The dotted lines represent a continuation of bridging oxygen bonds across the surface.The proposed reactions ((a) and (b))can explain the observed decreasing surface potential at pH < 4, since these types of surface reactions are crowding out H+ (therefore decreasing surface charge). At higher pH, in the case of –COO–groups at the pH > 4 ((c) and (d) -malonate anions), the preferred type of association is bidentate dissociated inner sphere complex. This type of binding does not significantly change the surface charge, therefore neither its potential.

Author Contributions: Conceptualization, P.Z., K.K.; methodology, K.K., T.B., W.P. formal analysis, K.K., T.B., D.N., K.L., P.Z.; investigation, K.K., K.L., D.N., M.Ł.; resources, K.K., T.B., W.P.; writing-original draft preparation, K.K., T.B., K.L., D.N., P.Z.; writing—review and editing, K.K., T.B., P.Z., D.N., K.L.; visualization, K.K., D.N., P.Z.; supervision, K.K., T.B., W.P., P.Z.; project administration, K.K.; All authors have read and agreed to the published version of the manuscript.

Funding: This research was funded by by the NCN Grant Sonata Bis (UMO-2016/22/E/ST4/00446). And P.Z. was supported by the U.S. Department of Energy (DOE) Chemical Sciences, Geosciences, and Biosciences Division under Contract DE-AC02-05CH11231.

Institutional Review Board Statement: Not applicable.

Acknowledgments: This work was supported by the NCN Grant Sonata Bis (UMO-2016/22/E/ST4/00446). P.Z. was supported by the U.S. Department of Energy (DOE) Chemical Sciences, Geosciences, and Biosciences Division under Contract DE-AC02-05CH11231. The following are available online at https://www.mdpi.com/article/10.3390/colloids5040047/s1, Supplement.

Conflicts of Interest: The authors declare no conflict of interest.

References

1. Scalenghe, R. *Soils: Basic Concepts and Future Challenges*; Certini, G., Scalenghe, R., Eds.; Cambridge University Press: Cambridge, UK, 2006; Volume 9780521851, ISBN 9780511535802.
2. Kleber, M.; Eusterhues, K.; Keiluweit, M.; Mikutta, C.; Mikutta, R.; Nico, P.S. Mineral–Organic Associations: Formation, Properties, and Relevance in Soil Environments. In *Advances in Agronomy*; Academic Press: Cambridge, MA, USA, 2015; Volume 130, pp. 1–140.
3. Kögel-Knabner, I.; Guggenberger, G.; Kleber, M.; Kandeler, E.; Kalbitz, K.; Scheu, S.; Eusterhues, K.; Leinweber, P. Organo-mineral associations in temperate soils: Integrating biology, mineralogy, and organic matter chemistry. *J. Plant Nutr. Soil Sci.* **2008**, *171*, 61–82. [CrossRef]
4. Chen, C.; Hall, S.J.; Coward, E.; Thompson, A. Iron-mediated organic matter decomposition in humid soils can counteract protection. *Nat. Commun.* **2020**, *11*, 2255. [CrossRef]
5. Wagai, R.; Kajiura, M.; Asano, M. Iron and aluminum association with microbially processed organic matter via meso-density aggregate formation across soils: Organo-metallic glue hypothesis. *Soil* **2020**, *6*, 597–627. [CrossRef]
6. Kleber, M.; Bourg, I.C.; Coward, E.K.; Hansel, C.M.; Myneni, S.C.B.; Nunan, N. Dynamic interactions at the mineral–organic matter interface. *Nat. Rev. Earth Environ.* **2021**, *2*, 402–421. [CrossRef]
7. Kleber, M.; Sollins, P.; Sutton, R. A conceptual model of organo-mineral interactions in soils: Self-assembly of organic molecular fragments into zonal structures on mineral surfaces. *Biogeochemistry* **2007**, *85*, 9–24. [CrossRef]
8. Kramer, M.G.; Chadwick, O.A. Climate-driven thresholds in reactive mineral retention of soil carbon at the global scale. *Nat. Clim. Chang.* **2018**, *8*, 1104–1108. [CrossRef]
9. Torn, M.S.; Trumbore, S.E.; Chadwick, O.A.; Vitousek, P.M.; Hendricks, D.M. Mineral control of soil organic carbon storage and turnover. *Nature* **1997**, *389*, 170–173. [CrossRef]
10. Jones, D.L. Organic acids in the rhizosphere—A critical review. *Plant Soil* **1998**, *205*, 25–44. [CrossRef]
11. Kawamura, K.; Ono, K.; Tachibana, E.; Charriére, B.; Sempéré, R. Distributions of low molecular weight dicarboxylic acids, ketoacids and α-dicarbonyls in the marine aerosols collected over the Arctic Ocean during late summer. *Biogeosciences* **2012**, *9*, 4725–4737. [CrossRef]
12. Kallay, N.; Dojnović, Z.; Čop, A. Surface potential at the hematite-water interface. *J. Colloid Interface Sci.* **2005**, *286*, 610–614. [CrossRef]
13. Preočanin, T.; Čop, A.; Kallay, N. Surface potential of hematite in aqueous electrolyte solution: Hysteresis and equilibration at the interface. *J. Colloid Interface Sci.* **2006**, *299*, 772–776. [CrossRef]
14. Zarzycki, P.; Chatman, S.; Preočanin, T.; Rosso, K.M. Electrostatic potential of specific mineral faces. *Langmuir* **2011**, *27*, 7986–7990. [CrossRef] [PubMed]
15. Zarzycki, P.; Rosso, K.M.; Chatman, S.; Preočanin, T.; Kallay, N.; Piasecki, W. Theory, experiment and computer simulation of the electrostatic potential at crystal/electrolyte interfaces. *Croat. Chem. Acta* **2010**, *83*, 457–474.
16. Preočanin, T.; Kallay, N. Effect of electrolyte on surface potential of haematite in aqueous electrolyte solutions. *Surf. Eng.* **2008**, *24*, 253–258. [CrossRef]
17. Yanina, S.V.; Rosso, K.M. Linked Reactivity at Mineral-Water Interfaces Through Bulk Crystal Conduction. *Science* **2008**, *320*, 218–222. [CrossRef]
18. Chatman, S.; Zarzycki, P.; Rosso, K.M. Surface potentials of (001), (012), (113) hematite (α-Fe_2O_3) crystal faces in aqueous solution. *Phys. Chem. Chem. Phys.* **2013**, *15*, 13911–13921. [CrossRef]
19. Shimizu, K.; Boily, J.-F. Electrochemical Properties and Relaxation Times of the Hematite/Water Interface. *Langmuir* **2014**, *30*, 9591–9598. [CrossRef]
20. Shimizu, K.; Boily, J.-F. Electrochemical Signatures of Crystallographic Orientation and Counterion Binding at the Hematite/Water Interface. *J. Phys. Chem. C* **2015**, *119*, 5988–5994. [CrossRef]
21. Shimizu, K.; Nyström, J.; Geladi, P.; Lindholm-Sethson, B.; Boily, J.-F. Electrolyte ion adsorption and charge blocking effect at the hematite/aqueous solution interface: An electrochemical impedance study using multivariate data analysis. *Phys. Chem. Chem. Phys.* **2015**, *17*, 11560–11568. [CrossRef]
22. Preočanin, T.; Janusz, W.; Kallay, N. Evaluation of equilibrium parameters of the anatase/aqueous electrolyte solution interface by introducing surface potential data. *Colloids Surf. A Physicochem. Eng. Asp.* **2007**, *297*, 30–37. [CrossRef]
23. Kallay, N.; Preočanin, T.; Šupljika, F. Measurement of surface potential at silver chloride aqueous interface with single-crystal AgCl electrode. *J. Colloid Interface Sci.* **2008**, *327*, 384–387. [CrossRef] [PubMed]
24. Lützenkirchen, J.; Preočanin, T.; Kovačević, D.; Tomišić, V.; Lövgren, L.; Kallay, N. Potentiometric Titrations as a Tool for Surface Charge Determination. *Croat. Chem. Acta* **2012**, *85*, 391–417. [CrossRef]

25. Preočanin, T.; Namjesnik, D.; Klačić, T.; Šutalo, P. The Effects on the Response of Metal Oxide and Fluorite Single Crystal Electrodes and the Equilibration Process in the Interfacial Region. *Croat. Chem. Acta* **2017**, *90*, 333–344. [CrossRef]
26. *Determination of Organic Structures by Physical Methods*, 1st ed.; Braude, E.A.; Nachod, F.C. (Eds.) Academic Press Inc.: New York, NY, USA, 1955; ISBN 9781483275727.
27. Szymanek, K.; Charmas, R.; Piasecki, W. A study on the mechanism of Ca^{2+} adsorption on TiO_2 and Fe_2O_3 with the usage of calcium ion-selective electrode. *Chemosphere* **2020**, *242*, 125162. [CrossRef]
28. Piasecki, W.; Szymanek, K.; Charmas, R. Fe^{2+} adsorption on iron oxide: The importance of the redox potential of the adsorption system. *Adsorption* **2019**, *25*, 613–619. [CrossRef]
29. Jonsson, C.M.; Jonsson, C.L.; Sverjensky, D.A.; Cleaves, H.J.; Hazen, R.M. Attachment of L-glutamate to rutile (α-TiO_2): A Potentiometric, adsorption, and surface complexation study. *Langmuir* **2009**, *25*, 12127–12135. [CrossRef]
30. *Aquatic Chemical Kinetics—Reaction Rates of Processes in Natural Waters*; Stumm, W. (Ed.) John Wiley & Sons, Inc.: Hoboken, NJ, USA, 1991; Volume 152, ISBN 0471510297.
31. Sposito, G. On Points of Zero Charge. *Environ. Sci. Technol.* **1998**, *32*, 2815–2819. [CrossRef]
32. Preočanin, T.; Kallay, N. Evaluation of surface potential from single crystal electrode potential. *Adsorption* **2013**, *19*, 259–267. [CrossRef]
33. Kedra-Królik, K.; Rosso, K.M.; Zarzycki, P. Probing size-dependent electrokinetics of hematite aggregates. *J. Colloid Interface Sci.* **2017**, *488*, 218–224. [CrossRef]
34. Toczydłowska, D.; Kedra-Królik, K.; Nejbert, K.; Preočanin, T.; Rosso, K.M.; Zarzycki, P. Potentiometric and electrokinetic signatures of iron(ii) interactions with (α,γ)-Fe2O3. *Phys. Chem. Chem. Phys.* **2015**, *17*, 26264–26269. [CrossRef]
35. Zarzycki, P.; Preočanin, T. Point of zero potential of single-crystal electrode/inert electrolyte interface. *J. Colloid Interface Sci.* **2012**, *370*, 139–143. [CrossRef] [PubMed]
36. Zarzycki, P. Comparison of the Monte Carlo estimation of surface electrostatic potential at the hematite (0 0 0 1)/electrolyte interface with the experiment. *Appl. Surf. Sci.* **2007**, *253*, 7604–7612. [CrossRef]
37. Kosmulski, M. Isoelectric points and points of zero charge of metal (hydr)oxides: 50 years after Parks' review. *Adv. Colloid Interface Sci.* **2016**, *238*, 1–61. [CrossRef] [PubMed]
38. Duckworth, O.W.; Martin, S.T. Surface complexation and dissolution of hematite by C1-C6 dicarboxylic acids at pH = 5.0. *Geochim. Cosmochim. Acta* **2001**, *65*, 4289–4301. [CrossRef]
39. Litter, M.I.; Villegas, M.; Blesa, M.A. Photodissolution of iron oxides in malonic acid. *Can. J. Chem.* **1994**, *72*, 2037–2043. [CrossRef]
40. Zarzycki, P.; Charmas, R.; Piasecki, W. Formal mathematical analysis of the existence of the common intersection point in relation to determining the parameters describing ion adsorption at the oxide/electrolyte interface: Comparison of the triple and four-layer models. *Adsorption* **2004**, *10*, 139–149. [CrossRef]
41. Kallay, N.; Preocanin, T.; Ivsić, T. Determination of surface potentials from the electrode potentials of a single-crystal electrode. *J. Colloid Interface Sci.* **2007**, *309*, 21–27. [CrossRef]
42. Zarzycki, P.; Rosso, K.M. Nonlinear response of the surface electrostatic potential formed at metal oxide/electrolyte interfaces. A Monte Carlo simulation study. *J. Colloid Interface Sci.* **2010**, *341*, 143–152. [CrossRef]
43. Persson, P.; Axe, K. Adsorption of oxalate and malonate at the water-goethite interface: Molecular surface speciation from IR spectroscopy. *Geochim. Cosmochim. Acta* **2005**, *69*, 541–552. [CrossRef]
44. Lenhart, J.J.; Bargar, J.R.; Davis, J.A. Spectroscopic evidence for ternary surface complexes in the lead(II)-malonic acid-hematite system. *J. Colloid Interface Sci.* **2001**, *234*, 448–452. [CrossRef] [PubMed]
45. Soltis, J.A.; Schwartzberg, A.M.; Zarzycki, P.; Penn, R.L.; Rosso, K.M.; Gilbert, B. Electron Mobility and Trapping in Ferrihydrite Nanoparticles. *ACS Earth Space Chem.* **2017**, *1*, 216–226. [CrossRef]
46. Katz, J.E.; Zhang, X.; Attenkofer, K.; Chapman, K.W.; Frandsen, C.; Zarzycki, P.; Rosso, K.M.; Falcone, R.W.; Waychunas, G.A.; Gilbert, B. Electron small polarons and their mobility in iron (oxyhydr)oxide nanoparticles. *Science* **2012**, *337*, 1200–1203. [CrossRef] [PubMed]
47. Mangiante, D.M.; Schaller, R.D.; Zarzycki, P.; Banfield, J.F.; Gilbert, B. Mechanism of Ferric Oxalate Photolysis. *ACS Earth Space Chem.* **2017**, *1*, 270–276. [CrossRef]